PAPER

NJC
www.rsc.org/njc

Selectivity in C–Cl bond activation of dichloroarenes by photogenerated Cp*Re(CO)$_2$: combined experimental and DFT studies

Alvaro Aballay,[a] Eric Clot,[b] Odile Eisenstein,*[b] Maria Teresa Garland,[c] Fernando Godoy,[a] A. Hugo Klahn,*[a] Juan Carlos Muñoz[c] and Beatriz Oelckers[a]

[a] *Instituto de Quimica, Pontificia Universidad Catolica de Valparaiso, Casilla 4059 Valparaiso, Chile. E-mail: hklahn@ucv.cl*
[b] *Laboratoire de Structure et Dynamique des Systèmes Moléculaires et Solides (CNRS UMR 5636), Université Montpellier 2, Case courrier 14, 34095 Montpellier cedex 5, France. E-mail: odile.eisenstein@univ-montp2.fr*
[c] *CIMAT, Facultad de Ciencias Fisicas y Matematicas, Universidad de Chile, Casilla 653 Santiago, Chile*

Received (in Montpellier, France) 5th July 2004, Accepted 13th September 2004
First published as an Advance Article on the web 9th December 2004

The photochemical reaction of the d^6 Re(I) complex Cp*Re(CO)$_3$ with several substituted dichloroarenes (1-R-2,4-dichlorobenzene; R = Me, OMe, CF$_3$ and F) yields the insertion products *trans*-Cp*Re(CO)$_2$(C$_6$H$_3$ClR)Cl. The C–Cl bond activation of 2,4-dichloroanisole and 2,4-dichloro-1-fluorobenzene occurs at position 2 (*ortho* to the methoxy and fluoro substituents, respectively), whereas for 2,4-dichlorotoluene and 2,4-dichloro-1-trifluoromethylbenzene the C–Cl bond in position 4 (*para* to the Me and CF$_3$ groups, respectively) is cleaved. The products have been characterized by elemental analyses and spectroscopic techniques, and by X-ray crystallography for the complexes *trans*-Cp*Re(CO)$_2$(5-chloro-2-methoxyphenyl)Cl and *trans*-Cp*Re(CO)$_2$(3-chloro-4-methylphenyl)Cl. DFT(B3PW91) calculations have been carried out to explain the selectivity observed in the isolated insertion products. It is shown that the Re–aryl bond dissociation energy is stronger in the observed isomer. This is analyzed as originating from a combination of electronic and steric factors.

Introduction

The transformation of chloroarenes mediated by transition metal complexes is a field of major interest. Chloroarenes, normally less reactive than their brominated and iodinated counterparts, are nevertheless preferred precursors for C–C coupling reactions (Heck, Suzuki, Sonogashira, Stille) because of their much lower cost.[1] Another application is halocarbon degradation for environmental remediation.[2] For these reasons, considerable attention has been focused on the transition metal catalyzed dechlorination of aryl chlorides.[3] A large number of stoichiometric and catalytic reactions have been reported, particularly with d^8 and d^{10} transition metal species,[4–10] but fewer with d^6 metal systems.[11–13]

Selective dechlorination of polychlorobenzene compounds by homogeneous catalysis is highly dependent on the position of the chlorine in the aromatic ring and also on the nature of the catalyst. For example, 1,2,4-trichlorobenzene can be monodehalogenated by RhH$_2$Cl(PPr$^i_3$)$_2$[14] and RhCl(PPh$_3$)$_3$[15,16] to give exclusively 1,2-dichlorobenzene, whereas the same substrate reacted with Ni(PEt$_3$)$_4$ produces only a stable 2,5-dichlorophenyl nickel complex, *trans*-NiCl(2,5-Cl$_2$C$_6$H$_3$)(PEt$_3$)$_2$.[4] On the other hand, several other complexes of Pd(II),[17] Ni(0),[18] Ni(II),[19] Ru(II)[14] yield mixtures of dichlorobenzene in the degradation of 1,2,4-trichlorobenzene. There is little information on the dechlorination of substituted chloroarenes. Electron-donating (Me, OMe, NH$_2$) or electron-withdrawing (COOH, MeCO, CF$_3$) groups have no effect on the hydrogenolysis of 3- and 4-substituted chlorobenzenes using RhL$_2$HCl$_2$ (L = PCy$_3$, PPr$^i_3$).[20] In all cases, an almost quantitative yield of the corresponding arene was obtained whatever the substitution pattern. However, while 3- and 4-chlorotoluenes are almost equally reactive, affording toluene in more than 90% yield, reaction of 2-chlorotoluene under the same conditions produces toluene in 7% yield only. The protecting steric factor of the methyl group was claimed to be responsible for this result. However, no steric effects were observed in the degradation reaction of 2-chlorotoluene and 2,6-dichlorotoluene catalyzed by (Cp*RhCl$_2$)$_2$, where Cp* = η^5-C$_5$Me$_5$.[21] In both cases, toluene was formed in high yields, 92% and 96%, respectively. Similarly, 2,3-dichloronitrobenzene can be selectively dechlorinated by Pd(PPh$_3$)$_4$ to give 3-chloronitrobenzene in 94% yield.[22] Recently, we have also observed the selective insertion of the photogenerated fragment Cp*Re(CO)$_2$ into the C–Cl bonds of 2,4,5-trichloroanisole and 3,4,5-trichloro-1-trifluoromethylbenzene to form the complexes Cp*Re(CO)$_2$(aryl^{Cl})Cl, where aryl^{Cl} = 4,5-dichloro-2-methoxyphenyl and 2,3-dichloro-5-trifluoromethylphenyl, respectively.[23]

To better understand these apparently contradictory results we have studied the photochemical reactions of the d^6 Re(I) complex Cp*Re(CO)$_3$ with several substituted dichloroarenes (1-R-2,4-Cl$_2$C$_6$H$_3$, R = Me, OMe, CF$_3$ and F). Our goal is to establish how the steric and/or electronic effects of the benzene substituents influence the insertion of the photogenerated rhenium fragment into the different C–Cl bonds of the substrate. DFT calculations have been used to discuss the selectivity observed in the isolated insertion products.

DOI: 10.1039/b410265g

Results and discussion

Experimental results

The complexes of the general formula Cp*Re(CO)$_2$(C$_6$H$_3$ClR)Cl (R = OMe, F, CF$_3$, Me), **1**–**4**, were prepared by UV irradiation (λ = 350 nm) of Cp*Re(CO)$_3$ in neat 2,4-dichlorotoluene, 2,4-dichloro-1-trifluoromethylbenzene and 2,4-dichoro-1-fluorobenzene, or in a saturated hexane solution of 2,4-dichloroanisole, as shown in Scheme 1. Much longer irradiation times or irradiation at λ = 300 nm did not increase the yields of the products: instead, it led to the additional formation of Cp*Re(CO)$_2$Cl$_2$.[13] These complexes were purified by column chromatography and isolated as red microcrystalline solids after recrystallization from CH$_2$Cl$_2$ and hexane. In all cases, the compounds were obtained as a single isomer with the chloroaryl group *trans* to the chloride ligand. These new complexes have been identified by IR, ^{1}H NMR, ^{13}C NMR, and mass spectroscopies, elemental analysis and, in two cases, by X-ray crystallography (*vide infra*).

The IR spectra of **1**–**4** exhibited two ν(CO) absorptions around 2040 and 1960 cm^{-1}. The higher wavenumber stretching mode (ν_s) has a weaker intensity than the lower wavenumber stretching mode (ν_{as}). Similar intensity patterns have been observed in several other dicarbonyl rhenium complexes.[13,24] The appearance of a single resonance for the CO groups in the ^{13}C NMR spectra near 195 ppm is further evidence of the *trans* orientation of these ligands.[13] The ^{1}H NMR spectra of complexes **1**–**4** supports the formation of only one insertion product, since they exhibit a single resonance for the Cp* ligand. In addition, **1** and **4** show resonances for the protons of the OCH$_3$ and CH$_3$ substituents of the aryl ligand. In all cases, the aromatic region clearly shows the presence of three distinguishable proton environments with an integration ratio of 1 : 1 : 1. Complexes **1**–**4** are stable in the solid state at room temperature with respect to *trans*-*cis* isomerization. However, some *trans*-*cis* interconversion takes place in CDCl$_3$ solution for **3** and **4** as shown by small intensity resonances in the ^{1}H NMR spectra (*cis* : *trans* ratio of 1 : 13 for **3** and 1 : 24 for **4**, obtained by integration of the Cp* resonances).

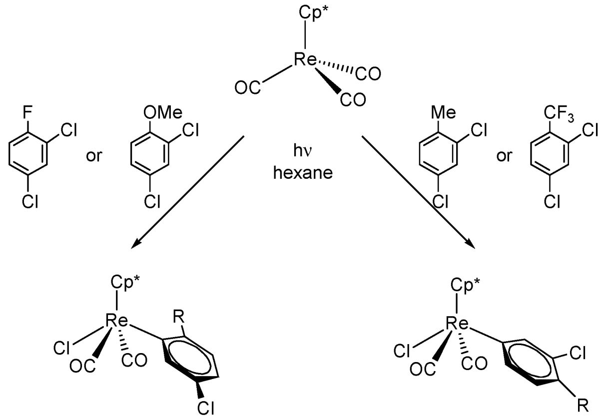

1 R = OMe
2 R = F

3 R = Me
4 R = CF$_3$

Scheme 1 Products from the irradiation of Cp*Re(CO)$_3$ at λ = 350 nm in the presence of different dichlorobenzene compounds.

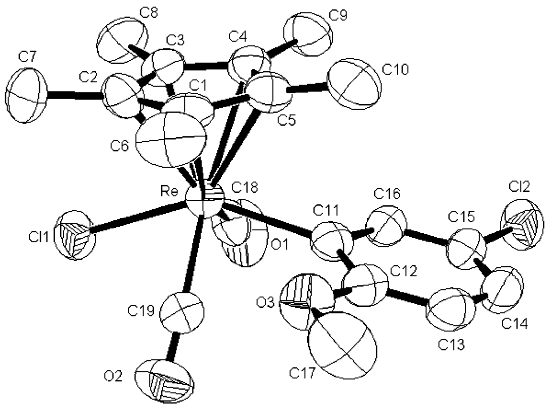

Fig. 1 Molecular structure of complex *trans*-Cp*Re(CO)$_2$[C$_6$H$_3$Cl(OCH$_3$)]Cl (**1**) drawn with 50% probability displacement ellipsoids. Only one independent molecule of the two present in the crystal is shown.

The insertion product of the rhenium fragment Cp*Re(CO)$_2$ into one of the two distinct C–Cl bonds of the dichloroarene was assigned by comparing the chemical shifts of the aromatic protons of the chloroaryl ligand of the resulting oxidative addition product to the aromatic proton chemical shifts of the free substrate. Insertion of the rhenium fragment is expected to unshield the protons at the *ortho* position.[25,26] For complexes **1** and **2**, only one aromatic proton resonance is shifted to lower field, indicating that the C–Cl bond at the 2-position has been cleaved, whereas for complexes **3** and **4**, two aromatic protons are shifted to lower field as a result of the cleavage of the C–Cl bond at position 4. This assignment was confirmed by ^{1}H–^{1}H NOESY experiments on complexes **1** and **3**. **1** showed a unique NOE interaction between the Cp* protons and the lower field aromatic protons but **3** exhibited two NOE interactions between the Cp* protons and the lower field aromatic resonances, as expected. Additional experimental evidence for the cleavage of a C–halogen bond at the 2-position was obtained from the photochemical reaction of Cp*Re(CO)$_3$ in a saturated solution of 2-bromo-4-chloroanisole. The product *trans*-Cp*Re(CO)$_2$[C$_6$H$_3$Cl(OMe)]Br, expected from the lower dissociation energy of the C–Br *vs.* C–Cl bonds, shows almost identical aromatic chemical shifts as observed for **1**. The ^{19}F NMR spectrum of complex **2** also confirms the above assignment, since the resonance at δ −78.6 ppm is in good agreement with reported values for similar complexes containing an aryl ligand with *ortho* fluorine groups.[26] Furthermore, X-ray crystallographic analyses of **1** (Fig. 1) and **4** (Fig. 2) confirm cleavage of the C–Cl bond *ortho* and *para* to the OMe and Me substituents, respectively. Table 1 reports crystal structure and refinement data and Table 2 shows selected bond distances and angles. In both complexes the rhenium atoms are seven-coordinate, with the Cp* ligand as a three-coordinate monoanion, and the overall geometry is comparable to a four-legged piano stool, which is consistent with a Re^{III} oxidation state. In general, bond distances and angles for complexes **1** and **4** compare with those of *trans*-Cp*Re(CO)$_2$(2,3,4,5-Cl$_4$C$_6$H)Cl [13] and *trans*-Cp*Re(CO)$_2$(4,5-Cl$_2$-2-OMeC$_6$H$_2$)Cl.[23] The Re–Cp* (centroid) distance of 1.962 and 1.966 Å for **1** and **4**, respectively, as well as the C–O bond lengths are similar to those determined in other cyclopentadie-

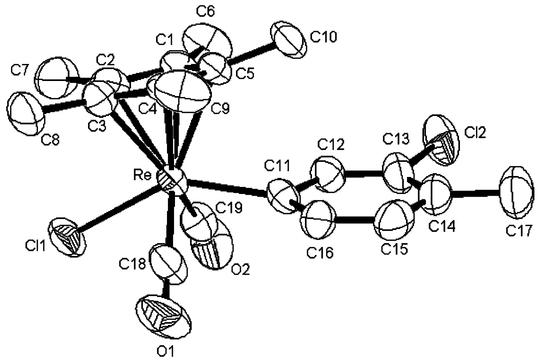

Fig. 2 Molecular structure of complex *trans*-Cp*Re(CO)$_2$(C$_6$H$_3$ClCH$_3$)Cl (**4**) drawn with 50% probability displacement ellipsoids.

Table 1 Crystallographic data for **1** and **4**

	1	**4**
Formula	$C_{19}H_{21}Cl_2O_3Re$	$C_{19}H_{21}Cl_2O_2Re$
MW/g mol^{-1}	559.46	538.46
Temperature/K	297(2)	297(2)
Crystal system	Monoclinic	Orthorhombic
Space group	$P2_1/c$	$Pca2_1$
a/Å	28.259(3)	14.0448(12)
b/Å	8.4639(7)	8.5444(7)
c/Å	16.7535(15)	15.8837(14)
β/°	100.4730(10)	—
U/Å^3	3940.3(6)	1906.1(3)
Z	4	4
ρ_{calcd}/g cm^{-3}	1.869	1.876
μ/mm^{-1}	6.453	6.663
Reflections collected	27851	13222
Unique reflections	8817	4302
R(int)	0.0621	0.039
R_1 ($I > 2\sigma_I$)	0.0434	0.0287
wR_2 ($I > 2\sigma_I$)	0.0997	0.0546
R_1 (all data)	0.0649	0.0373
wR_2 (all data)	0.1108	0.0579

nyl rhenium complexes. The OC–Re–CO interbond angles of 99.3° for **1** and 99.5° for **4**, clearly establish the *trans* orientation of these ligands and are quite similar to those observed in several similar complexes.[13,23]

The most interesting feature is the selective insertion of the rhenium fragment into a C–Cl bond as a function of the substituent in position 1 in the 2,4-dichloroarenes. Fluoro and methoxy groups direct the C–Cl bond activation towards the 2-position, whereas methyl and trifluoromethyl substituents direct the reaction towards the 4-position. The *ortho* directing effect appears to be similar to that found in the C–H activation of hydrofluorobenzene systems by the same metal fragment.[25,26] We did not attempt to identify any products that could be formed by C–H bond activation or η^2-coordination of the dichloroarene, even though we have experimental evidence for η^2-coordination of chlorobenzenes to rhenium in the complexes Cp*Re(CO)$_2$(5,6-η^2-1,2,4-$Cl_3C_6H_3$) and Cp*Re(CO)$_2$(5,6-η^2-1,2,3,4-$Cl_4C_6H_2$).[27]

Table 2 Selected bond lengths (Å) and angles (°) for **1** and **4**

	1a[a]	**1b**[a]	**4**
Re–C(Cp*)	2.348(7)	2.355(7)	2.325(5)
Re–C(2)	2.298(7)	2.303(7)	2.275(6)
Re(1)–C(3)	2.261(7)	2.252(7)	2.261(6)
Re(1)–C(4)	2.289(7)	2.271(6)	2.317(7)
Re(1)–C(5)	2.344(7)	2.342(6)	2.345(5)
Re(1)–centroid Cp*	1.964	1.960	1.966
Re(1)–C(CO)	1.925(8)	1.908(8)	1.926(7)
Re(1)–C(CO)	1.968(8)	1.960(9)	1.948(7)
Re(1)–C(11)	2.189(7)	2.185(6)	2.174(8)
Re(1)–Cl(1)	2.4804(19)	2.4723(19)	2.4717(13)
C(18)–O(1)	1.148(9)	1.145(9)	1.145(7)
C(19)–O(2)	1.131(9)	1.133(9)	1.135(8)
C(18)–Re(1)–C(19)	99.3(3)	100.4(3)	99.5(3)
C(11)–Re(1)–Cl(1)	144.07(17)	143.26(17)	143.5(2)

[a] Two independent molecules of **1** are found in the unit cell and labeled as **1a** and **1b**.

Table 3 Relative energy (ΔE/kJ mol^{-1}) of CpRe(CO)$_2$(2-R-5-ClC_6H_3)Cl, *ortho*, relative to CpRe(CO)$_2$(4-R-3-ClC_6H_3)Cl, *para*. Bond dissociation energies (BDE in kJ mol^{-1}) of C–Cl in 1-R-2,4-$Cl_2C_6H_3$ and Re–C in CpRe(CO)$_2$(C_6H_3ClR)Cl.[a]

R	ΔE[b]	BDE(Cl–C) *ortho*	BDE(Cl–C) *para*	BDE(Re–C) *ortho*	BDE(Re–C) *para*
CF_3	−14.2	377.7	387.7	212.4	236.4
F	+21.9	387.9	388.3	258.0	236.4
Me	−22.5	387.8	389.4	210.5	234.6
OMe	+10.0	388.1	391.3	245.0	238.2

[a] Here *ortho* (resp. *para*) indicates that the carbon of the C–Cl and Re–C bonds is *ortho* (resp. *para*) to R. [b] A positive value for ΔE corresponds to a higher stability of the *ortho* isomer.

Computational studies

Insertion products of the CpRe(CO)$_2$ fragment into the C–Cl bond of 1-R-2,4-$Cl_2C_6H_3$ were optimized with DFT(B3PW91) calculations. The relative energies of the products (Table 3) nicely agree with the experimental observations. The OMe and F substituents direct the insertion into the *ortho* C–Cl bond whereas Me and CF_3 show a preference for insertion into the *para* C–Cl bond. The differences in energy are small, showing a subtle influence of the substituent on the insertion pattern. No attempt was made to locate the transition states for insertion so that these computational results only reflect the stability preferences of the two possible insertion products. The calculations were also limited to the observed *trans* isomers. A study of the reaction energy profile such as the one performed on the insertion of CpRe(CO)$_2$ into the C–H bond of hydrofluorobenzene systems[28] will be necessary to fully analyze the factors that control the formation of the regioisomers; this will be carried out in future work.

The calculated geometries (Table 4) of the complexes are in good agreement with the structural data measured by X-ray crystallography (Table 2). The overall piano-stool structure is well reproduced with average angles of 145° and 98° for C(aryl)–Re–Cl and C(O)–Re–C(O), respectively. The phenyl ring is parallel to the Cp ring in all cases. The bond distances are also in good agreement with the experimental values. For instance, in the case of the OMe group *ortho* to the Re fragment, **1**, and the associated calculated model, the Re–C(aryl) bond is 2.198 Å (calcd) *versus* 2.189(7) Å (exp.). In the case of the Me group *para* to the rhenium fragment, **4**, the Re–C(aryl) bond is 2.193 Å (calcd), which is longer than the experimental value of 2.174(8) Å, but still within the experimental limits taking into account the e.s.d.

The calculations show only a moderate influence of the nature of R on the metric parameters. However, an interesting trend appears when comparing the *ortho* and *para* regioisomers (Table 4). For any R substituent, the Re–C(aryl) bond is shorter when R is in the *para* position, the difference in bond length being negligible in the case of R = F. This trend can be better explained on steric grounds, which are especially important for CH_3 and CF_3 and minimal in the case of F. It thus appears that the Re–C(aryl) bond length is not a good parameter to account for the structural preferences.

To understand the regiochemistry, we compared the Re–C bond dissociation energy (BDE) with the corresponding C–Cl BDE in the original R-substituted dichloroarene molecules (Table 3). Without exception, the Re–C bond is stronger in the rhenium complex that is preferred experimentally by 7 to 20 kJ mol^{-1}. However, the pattern is less clear in the reactant. The radical $C_6H_3ClR^{\bullet}$ is more stable when the carbon bearing the radical center is *ortho* to R (Table 3) because this allows a greater distance between the two large groups R and Cl. Therefore, in the case of OMe the weaker C–Cl bond is cleaved. In the case of Me and CF_3, the strongest C–Cl bond is cleaved while there is almost no difference between the two C–Cl bond dissociation energies in the case of F. The small differences in the C–Cl BDEs indicate that the two isomeric R-substituted chlorophenyl radicals have similar energies.

Table 4 Selected bond distances (Å) and angles (degrees) for *trans*-CpRe(CO)$_2$(2-R-5-ClC$_6$H$_3$)Cl (*ortho*) and *trans*-CpRe(CO)$_2$(4-R-3-ClC$_6$H$_3$)Cl (*para*) computed at the B3PW91 level. The numbering scheme is the same as the one used for the X-ray structures. The antisymmetric, ν_{as}(CO), and symmetric, ν_s(CO), unscaled stretching frequencies (cm^{-1}) are also given.

	OMe		Me		F		CF$_3$	
	ortho	*para*	*ortho*	*para*	*ortho*	*para*	*ortho*	*para*
Re–C1	2.267	2.343	2.257	2.339	2.263	2.333	2.257	2.321
Re–C5	2.307	2.333	2.299	2.330	2.304	2.332	2.300	2.329
Re–C4	2.370	2.310	2.377	2.310	2.371	2.318	2.380	2.329
Re–C11	2.198	2.187	2.221	2.193	2.193	2.192	2.226	2.191
Re–C18	1.977	1.937	1.976	1.940	1.978	1.944	1.981	1.947
Re–C19	1.925	1.962	1.922	1.960	1.927	1.957	1.926	1.955
Re–Cl1	2.503	2.511	2.498	2.510	2.498	2.509	2.500	2.508
C18–O1	1.149	1.154	1.150	1.153	1.148	1.153	1.147	1.152
C19–O2	1.155	1.150	1.155	1.150	1.155	1.151	1.154	1.150
C18–Re–C19	98.7	98.8	96.4	99.1	99.3	99.1	96.7	99.4
C11–Re–Cl1	144.6	144.7	144.6	144.9	144.1	144.9	145.5	144.8
ν_{as}(CO)	2074.7	2077.7	2075.4	2080.2	2079.6	2082.2	2080.2	2084.9
ν_s(CO)	2140.8	2134.6	2135.8	2135.5	2146.5	2136.3	2149.1	2138.5

Therefore, the energy preference for one of the two Re–aryl isomers can only come from the interaction between rhenium and aryl radicals. This is illustrated by the significantly different Re–C BDE values for the two isomers. The Re–C bond is stronger for the preferred product, which comes from a combination of electronic and steric factors. It has been shown that the Re–C bond is significantly strengthened by the presence of an *ortho* fluorine.[25] The electronegative OMe group induces similar effect. The CF$_3$ group does not stabilize the neighbouring Re–C bond (the electronegative atom should be directly bonded to the aryl ring). In contrast, the steric influence of CF$_3$ destabilizes the isomer where CF$_3$ is *ortho* to the rhenium fragment. This leads to a weaker Re–C in this nonobserved isomer. The situation is similar with CH$_3$. This analysis shows how electronic and steric factors combine to control the nature of the final isomer. We have calculated the symmetrical and antisymmetrical ν(CO) stretching frequencies (Table 4). The relative frequencies do not correlate in a clear manner with the relative BDE, thus showing that the strength of the Re–C bond is not related with the electron-donating and/or -releasing ability of C$_6$H$_3$ClR. This contrasts with the systematic relationship found between H–C and M–C bond energies.[25,28–32] This shows that the bond energy relationship H–C/M–C cannot be generalized to Y–C/M–C with Y $\neq$ H and further studies are needed.

Conclusion

The photogenerated Cp*Re(CO)$_2$ fragment inserts specifically in one of the C–Cl bonds of substituted dichloroarenes of general formula 1-R-2,4-Cl$_2$C$_6$H$_3$. In the case of R = F and OMe, the metal fragment inserts in the C–Cl bond *ortho* to R. In the case of R = Me and CF$_3$, the metal fragment inserts in the C–Cl *para* to R. DFT calculations show that the observed compound is the more stable regioisomer. The calculations also show that the observed regioisomer corresponds to the stronger Re–C bond and not necessarily to the more stable C$_6$H$_3$ClR organic radical. In the case of R = F and OMe, the substituent strengthens an *ortho* Re–C bond. Such strengthening does not occur when R = CH$_3$ or CF$_3$ and steric factors disfavor the presence of a large metal fragment adjacent to R.

Experimental

Methods and materials

All reactions were carried out under nitrogen using standard Schlenk techniques. Cp*Re(CO)$_3$ was prepared as previously described.[33] 2,4-Dichlorotoluene, 2,4-dichloro-1-trifluoromethylbenzene and 2,4-dichloro-1-fluorobenzene were used as received (Aldrich). 2-Bromo-4-chloroanisole and 2,4-dichloroanisole were prepared in 85–90% yield from the corresponding phenols by Williamson syntheses.[34] Infrared spectra were recorded in solution (CaF$_2$ cell) on a Perkin Elmer FT-1605 spectrophotometer, ^{1}H and ^{13}C NMR spectra on Bruker AVANCE 400 and AMX 500 instruments. All ^{1}H NMR chemical shifts were referenced using the chemical shifts of residual solvent, ^{13}C chemical shifts to solvent peaks and ^{19}F chemical shifts to C$_6$F$_6$ at −162.9. Mass spectra were obtained at the Laboratorio de Servicios Analíticos, Universidad Católica de Valparaíso, and the Chemistry Department of the University of York, on a Shimadzu GC-MSA and a VG Autospec instrument, respectively, under electron impact mode at 70 eV. Elemental analyses were obtained at the Centro de Instrumentación, Pontificia Universidad Católica de Chile, Santiago, Chile.

Photolysis of Cp*Re(CO)$_3$ in the presence of chlorinated substrates: general procedure

All reactions were carried out under nitrogen at room temperature in a Pyrex tube (25 cm long, 1.5 cm external diameter) fitted with a rubber septum. Cp*Re(CO)$_3$ (typically 50–150 mg) was dissolved in 15–20 ml of the chlorinated solvent (for 2,4-dichlorotoluene, 2,4-dichloro-1-trifluoromethylbenzene, and 2,4-dichloro-1-fluorobenzene) or in 20 ml of a saturated solution of the solid chlorinated compound (for 2-bromo-4-chloroanisole and 2,4-dichloroanisole). Solutions were irradiated at 350 nm for the time indicated below in a Rayonet RPR-100 photochemical reactor to give yellow to greenish-brown solutions. Solvent was removed under vacuum and the residue was chromatographed on silica gel 60 (Fluka).

***trans*-Cp*Re(CO)$_2$[C$_6$H$_3$Cl(OCH$_3$)]Cl.** (**1**) Irradiation time: 15 h. Cp*Re(CO)$_3$: 600 mg, 1.48 mmol. Following the general procedure, elution with hexane gave a mixture of reusable unreacted Cp*Re(CO)$_3$ and 2,4-dichloroanisole. Hexane–CH$_2$Cl$_2$ (3 : 1) eluted orange **1**, contaminated with traces of *trans*-Cp*Re(CO)$_2$Cl$_2$. **1** was isolated as pure orange crystals by layering a concentrated CH$_2$Cl$_2$ solution with hexane (yield 68 mg, 0.12 mmol, 8% conversion). IR (CH$_2$Cl$_2$) ν(CO)/cm^{-1}: 2040 s and 1954 vs; ^{1}H NMR (CDCl$_3$) δ: 1.71 (s, 15H), 3.80 (s, 3H), 6.73 (d, 1H, J = 8.6 Hz), 7.10 (dd, 1H, J = 8.6, 2.5 Hz), 7.65 (d, 1H, J = 2.5 Hz); ^{13}C–{^{1}H} NMR (CDCl$_3$) δ: 9.49 (C$_5$*Me*$_5$), 55.45 (OCH$_3$), 103.64 (*C*$_5$Me$_5$); 110.79 [C$_6$H$_3$Cl(OCH$_3$)], 120.07, 126.11, 126.63, 145.61, 162.65 [*C*$_6$H$_3$Cl(OCH$_3$)], 195.36 (CO); mass spectrum (based on ^{187}Re/^{35}Cl) m/z: 554 [M]$^+$, 526 [M − CO]$^+$, 498 [M − 2CO]$^+$, 356

[M – 2CO – $C_6H_3Cl(OCH_3)$]$^+$. Anal. calcd for $C_{19}H_{21}O_3Cl_2Re$: C, 41.16; H, 3.82%; found: C, 41.18; H, 3.75.

***trans*-Cp*Re(CO)$_2$[C$_6$H$_3$Cl(OCH$_3$)]Br.** Irradiation time: 6 h. Cp*Re(CO)$_3$: 150 mg, 0.37 mmol. Following the general procedure, elution with hexane eluted a mixture of unreacted Cp*Re(CO)$_3$ and 2-bromo-4-chloroanisole. Hexane–CH_2Cl_2 (2 : 1) eluted reddish-orange *trans*-Cp*Re(CO)$_2$[C$_6$H$_3$Cl(OCH$_3$)]Br, contaminated with traces of *trans*-Cp*Re(CO)$_2$Br$_2$. This complex was obtained pure as reddish-orange crystals by layering a concentrated CH_2Cl_2 solution of the impure solid with hexanes (yield 77 mg, 0.13 mmol). IR (CH_2Cl_2) ν(CO)/cm^{-1}: 2034 s and 1951 vs; ^{1}H NMR ($CDCl_3$) δ: 1.77 (s, 15H), 3.77 (s, 3H), 6.72 (d, 1H, J = 8.6 Hz), 7.10 (dd, 1H, J = 8.6, 2.5 Hz), 7.64 (d, 1H, J = 2.5 Hz); ^{13}C–{^{1}H} NMR ($CDCl_3$) δ: 9.93 ($C_5\mathit{Me}_5$), 55.47 ($O\mathit{C}H_3$), 103.18 (C_5Me_5); 110.81, 118.67, 126.03, 126.60, 145.42, 162.82 [$\mathit{C}_6H_3Cl(OCH_3)$], 193.99 (CO); mass spectrum (based on ^{187}Re/^{35}Cl) m/z: 598 [M]$^+$, 570 [M – CO]$^+$, 542 [M – 2CO]$^+$. Anal. calcd for $C_{19}H_{21}O_3BrClRe$: C, 38.10; H, 3.53%; found: C, 37.94; H, 3.41.

***trans*-Cp*Re(CO)$_2$(C$_6$H$_3$ClF)Cl.** (**2**) Irradiation time: 10 h. Cp*Re(CO)$_3$: 300 mg, 0.74 mmol. Following the general procedure, elution with hexane eluted unreacted Cp*Re(CO)$_3$ (205 mg, 0.51 mmol). Hexane–CH_2Cl_2 (5 : 1) eluted crude yellow **2**. This was crystallized by layering a concentrated CH_2Cl_2 solution with hexanes to give pure **2** (yield 82 mg, 0.14 mmol, 60%). IR (CH_2Cl_2) ν(CO)/cm^{-1}: 2044 s and 1963 vs; ^{1}H NMR ($CDCl_3$) δ: 1.78 (s, 15H), 6.95 (pst, 1H, J_{ap} = 8.6 Hz), 7.10 (m, 1H), 7.62 (dd, 1H, J_{HF} = 4.6 Hz, J_{HH} = 2.5 Hz). ^{13}C–{^{1}H} NMR ($CDCl_3$) δ: 9.51 (d, J_{CF} = 1 Hz, $C_5\mathit{Me}_5$), 103.99 (C_5Me_5); 115.03 (d, J_{CF} = 36 Hz, C_6H_3ClF), 115.93 (d, J_{CF} = 34 Hz, C_6H_3ClF), 127.45 (d, J_{CF} = 9.5 Hz, C_6H_3ClF), 129.28 (d, J_{CF} = 2.5 Hz, C_6H_3ClF), 145.54 (d, J_{CF} = 11 Hz, C_6H_3ClF), 166.92 (d, J_{CF} = 234 Hz, C_6H_3ClF), 194.39 (br s, CO); ^{19}F NMR ($CDCl_3$) δ −78.62 (m); mass spectrum (based on ^{187}Re/^{35}Cl) m/z: 542 [M]$^+$, 514 [M – CO]$^+$, 486 [M – 2CO]$^+$, 356 [M – 2CO – C_6H_3ClF]$^+$. Anal. calcd for $C_{18}H_{18}O_2Cl_2FRe$: C, 39.86; H, 3.34%; found: C, 39.96; H, 3.19.

***trans*-Cp*Re(CO)$_2$[C$_6$H$_3$Cl(CF$_3$)]Cl.** (**3**) Irradiation time: 14 h. Cp*Re(CO)$_3$: 200 mg, 0.49 mmol. Following the general procedure, elution with hexane gave 20 mg of a 1 : 2 mixture (according to ^{1}H NMR integration) of unreacted Cp*Re(CO)$_3$ and Cp*$_2$Re$_2$(CO)$_5$. Hexane–CH_2Cl_2 (2 : 1) eluted crude yellow **3**. Pure **3** was obtained as a yellow microcrystalline powder by layering a concentrated CH_2Cl_2 solution with hexane (yield 40 mg, 0.067 mmol, 14%). IR (CH_2Cl_2) ν(CO)/cm^{-1}: 2042 s and 1965 vs; ^{1}H NMR ($CDCl_3$) δ: 1.76 (s, 15H), 7.38 (d, 1H, J = 7.9 Hz), 7.61 (dd, 1H, J = 7.9, 1 Hz), 7.75 (d, 1H, J = 1 Hz); ^{13}C–{^{1}H} NMR ($CDCl_3$) δ: 9.47 ($C_5\mathit{Me}_5$), 103.84 (C_5Me_5); 128.78, 143.48, 147.20 [$\mathit{C}_6H_3Cl(CF_3)$], 196.86 (CO); other aromatic and CF_3 carbons could not be assigned due to isomerization to the *cis* isomer; ^{19}F NMR ($CDCl_3$) δ −62.54; mass spectrum (based on ^{187}Re/^{35}Cl) m/z: 592 [M]$^+$, 564 [M – CO]$^+$, 536 [M – 2CO]$^+$, 356 [M – 2CO – $C_6H_3Cl(CF_3)$]$^+$. Anal. calcd for $C_{19}H_{18}O_2Cl_2F_3Re$: C, 38.51; H, 3.04%; found: C, 38.50; H, 2.85.

***trans*-Cp*Re(CO)$_2$(C$_6$H$_3$ClCH$_3$)Cl.** (**4**) Irradiation time: 15 h. Cp*Re(CO)$_3$: 900 mg, 2.22 mmol. Following the general procedure, elution with hexane gave unreacted Cp*Re(CO)$_3$ (840 mg, 2.07 mmol). Hexane–CH_2Cl_2 (5 : 1) eluted orange **4** contaminated with traces of *trans*-Cp*Re(CO)$_2$Cl$_2$. Pure **4** was obtained as orange crystals by layering a concentrated CH_2Cl_2 solution with hexane (yield 30 mg, 0.056 mmol, 37%). IR (CH_2Cl_2) ν(CO)/cm^{-1}: 2034 s and 1955 vs; ^{1}H NMR ($CDCl_3$) δ: 1.72 (s, 15H), 2.33 (s, 3H), 6.96 (d, 1H, J = 7.7 Hz), 7.38 (dd, 1H, J = 7.7, 1.4 Hz), 7.55 (d, 1H, J = 1.4 Hz); ^{13}C–{^{1}H} NMR ($CDCl_3$) δ: 9.74 ($C_5\mathit{Me}_5$), 19.83 (CH_3), 103.80 (C_5Me_5); 124.71 [$\mathit{C}_6ClH_3(CH_3)$], 131.90, 133.16, 135.23, 143.94, 145.26 ($\mathit{C}_6H_3ClCH_3$), 197.29 (CO); mass spectrum (based on ^{187}Re/^{35}Cl) m/z: 538 [M]$^+$, 510 [M – CO]$^+$, 482 [M – 2CO]$^+$, 356 [M – 2CO – ($C_6H_3ClCH_3$)]$^+$. Anal. calcd for $C_{19}H_{21}O_2Cl_2Re$: C, 42.38; H, 3.93%; found: C, 42.33; H, 3.88.

Crystal structure determination

X-Ray quality crystals of **1** and **4** were obtained by recrystallization from solutions in hexanes by slow cooling to −10 °C. A summary of crystal data, data collection, and refinement parameters for the structural analyses is given in Table 1.† Crystals of **1** and **4** were glued to a glass fiber and mounted on a Bruker SMART APEX diffractometer, equipped with a CCD area detector. Data was collected using graphite-monochromated MoKα radiation (λ = 0.71073 Å). Cell constants for **1** and **4** were obtained from the least-squares refinement of three-dimensional centroids of 994 and 983 reflections, respectively, in the range $4.76° \le 2\theta \le 50.08°$. Data were measured through the use of CCD recording of ω rotation frames (0.3° each). All data were corrected for Lorentz and polarization effects. Absorption corrections were applied using the SADABS routine.[35] Both data were integrated with the Bruker SAINTPLUS program.[36]

The structures were solved by Patterson, completed by difference Fourier techniques and refined by full-matrix least-squares on F^2 (SHELXL-97)[37] with initial isotropic, but subsequent anisotropic thermal parameters. Hydrogens in **1** and **4** were included in calculated positions and refined riding on carbon atoms with free isotropic displacement parameters. Atomic scattering factors were used as implemented in the program.

Computational details

All calculations were performed with the Gaussian98 set of programs[38] within the framework of hybrid DFT (B3PW91),[39,40] on the model systems CpRe(CO)$_2$(C$_6$H$_3$ClR)Cl (Cp = η^5-C_5H_5; R = F, OMe, Me, CF_3). The rhenium atom was represented by the relativistic effective core potential (RECP) from the Stuttgart group (15 valence electrons) and its associated (8s7p6d)/[6s5p3d] basis set,[41] augmented by an f polarization function (α = 0.869).[42] The chlorine atoms were represented by RECP from the Stuttgart group and the associated basis set,[43] augmented by a d polarization function.[44] A 6-31G(d,p) basis set[45] was used for all the remaining atoms of the complex (C, H, O, F). Full optimizations of geometry without any constraints were performed, followed by analytical computation of the Hessian matrix to confirm the nature of the located extrema as minima on the potential energy surface. The arenes $C_6Cl_2H_3R$ and the radicals CpRe(CO)$_2$Cl and C_6H_3ClR (R = F, OMe, Me, CF_3) were optimized at the B3PW91 level (unrestricted formalism for open-shell systems) to estimate the Re–C and C–Cl BDEs.

Acknowledgements

We thank the Pontificia Universidad Católica de Valparaíso (DI 125782/02) and FONDECYT (Chile) for financial support (grant 1020655 and 7030107). B. O. acknowledges the Royal Society of Chemistry/CONICYT exchange program. O. E. thanks FONDECYT for an invited professorship to Pontificia

---

† CCDC reference numbers 244319 and 244320. See http://www.rsc.org/suppdata/nj/b4/b410265g/ for crystallographic data in .cif or other electronic format.

Universidad Católica de Valparaíso. We also wish to thank FONDAP (grant 1198002) and Fundacion Andes for financial support for the purchase of the X-ray diffractometer (Convenio C-13575) and the NMR spectrometer (Convenio C-13672). The donation of NH_4ReO_4 by MOLYMET-Chile was greatly appreciated.

References

1 (*a*) F. Lemaitre and P. Harvey, *J. Am. Chem. Soc.*, 2003, **125**, 5511; (*b*) B. M. Choudary, S. Mahdi, N. S. Chowdari, M. L. Kantam and B. Sreedar, *J. Am. Chem. Soc.*, 2002, **124**, 1427; (*c*) I. P. Beletskoya and A. V. Cheprokov, *Chem. Rev.*, 2000, **100**, 3009 and references therein.

2 A. Ghattas, R. Abu-Reziq, D. Avnir and J. Blum, *Green Chem.*, 2003, **5**, 40.

3 (*a*) V. V. Grushin and H. Alper, *Chem. Rev.*, 1994, **94**, 1047; (*b*) V. V. Grushin and H. Alper, *Top. Organomet. Chem.*, 1999, **3**, 193.

4 D. R. Fahey and J. E. Mahan, *J. Am. Chem. Soc.*, 1977, **99**, 2501.

5 L. M. Alcazar-Roman and J. F. Hartwig, *J. Am. Chem. Soc.*, 2001, **123**, 12905.

6 Y. Ben-David, M. Gozin, M. Portnoy and D. Milstein, *J. Mol. Catal.*, 1992, **73**, 173.

7 C. M. King, R. B. King, N. K. Bhattacharyya and M. G. Newton, *J. Organomet. Chem.*, 2000, **600**, 63.

8 Y. Akita, A. Inoue, K. Ishida, T. Terui and A. Ohta, *Synth. Commun.*, 1986, **16**, 1067.

9 A. Zapf and M. Beller, *Chem. Eur. J.*, 2001, **7**, 2908.

10 A. Spencer, *J. Organomet. Chem.*, 1984, **270**, 115.

11 C. Leiva and D. Sutton, *Organometallics*, 1998, **17**, 4568.

12 M. E. Cucullu, S. P. Nolan, T. R. Belderrain and R. H. Grubbs, *Organometallics*, 1999, **18**, 1299.

13 A. H. Klahn, A. Toro, B. Oelckers, G. E. Buono-Core, V. Manriquez and O. Wittke, *Organometallics*, 2000, **19**, 2580.

14 J. Diaz, M. A. Esteruelas, J. Herrero, L. Moraleja and M. Olivàn, *J. Catal.*, 2000, **195**, 187.

15 M. A. Esteruelas, J. Herrero, F. M. Lopez, M. Martin and L. A. Oro, *Organometallics*, 1999, **18**, 1110.

16 M. A. Atienza, M. A. Esteruelas, M. Fernandez, J. Herrero and M. Olivàn, *New J. Chem.*, 2001, **25**, 775.

17 L. Lassová, H. K. Lee and T. S. A. Hor, *J. Org. Chem.*, 1998, **63**, 3538.

18 D. R. Fahey, *J. Am. Chem. Soc.*, 1970, **92**, 402.

19 M. Stiles, *J. Org. Chem.*, 1994, **59**, 5381.

20 V. V. Grushin and H. Alper, *Organometallics*, 1991, **10**, 1620.

21 K.-I. Fujita, M. Owaki and R. Yamaguchi, *Chem. Commun.*, 2002, 2964.

22 A. Angeloff, J. J. Brunet, P. Legars, D. Neibecker and D. Souyri, *Tetrahedron Lett.*, 2001, **42**, 2301.

23 A. Aballay, F. Godoy, G. E. Buono-Core, A. H. Klahn, B. Oelckers, M. T. Garland and J. C. Muñoz, *J. Organomet. Chem.*, 2003, **688**, 168.

24 F. W. B. Einstein, A. H. Klahn, D. Sutton and K. G. Tyers, *Organometallics*, 1986, **5**, 53 and references therein.

25 E. Clot, M. Besora, F. Maseras, C. Mégret, O. Eisenstein, B. Oelckers and R. N. Perutz, *Chem. Commun.*, 2002, 490 and references therein.

26 J. J. Carbo, O. Eisenstein, C. L. Higgitt, A. H. Klahn, F. Maseras, B. Oelckers and R. N. Perutz, *J. Chem. Soc., Dalton Trans.*, 2001, 1452.

27 A. Abalay, A. H. Klahn and B. Oelckers, unpublished results.

28 E. Clot, B. Oelckers, A. H. Klahn, O. Eisenstein and R. N. Perutz, *Dalton Trans.*, 2003, 4065.

29 (*a*) W. D. Jones and E. T. Hessel, *J. Am. Chem. Soc.*, 1993, **115**, 554; (*b*) D. D. Wick and W. D. Jones, *Organometallics*, 1999, **18**, 495.

30 J. A. Martinho-Simões and J. L. Beauchamp, *Chem. Rev.*, 1990, **90**, 629.

31 H. E. Bryndza, L. K. Fong, R. A. Paciello, W. Tam and J. E. Bercaw, *J. Am. Chem. Soc.*, 1987, **109**, 1444.

32 P. L. Holland, R. A. Andersen, R. G. Bergman, J. Huang and S. P. Nolan, *J. Am. Chem. Soc.*, 1997, **119**, 128000.

33 A. T. Patton, C. E. Strouse, C. B. Knobler and J. A. Gladysz, *J. Am. Chem. Soc.*, 1983, **105**, 5804.

34 A. I. Vogel, *Vogel's Textbook of Practical Organic Chemistry*, Longman Group Limited, London, 4th edn., 1978, p. 754.

35 R. H. Blessing, *Acta Crystallogr., Sect. A*, 1995, **51**, 33.

36 (*a*) *SAINT+*, version 6.01, Bruker AXS, Inc., Madison, WI, USA, 2000; (*b*) *SAINT*, version 4.0, Bruker AXS, Inc., Madison, WI, USA, 2000.

37 G. M. Sheldrick, *SHELXL-97, Program for refinement of crystal structures*, University of Göttingen, Germany, 1997.

38 M. J. Frisch, G. W. Trucks, H. B. Schlegel, G. E. Scuseria, M. A. Robb, J. R. Cheeseman, V. G. Zakrzewski, J. A. Montgomery, Jr., R. E. Stratmann, J. C. Burant, S. Dapprich, J. M. Millam, A. D. Daniels, K. N. Kudin, M. C. Strain, O. Farkas, J. Tomasi, V. Barone, M. Cossi, R. Cammi, B. Mennucci, C. Pomelli, C. Adamo, S. Clifford, J. Ochterski, G. A. Petersson, P. Y. Ayala, Q. Cui, K. Morokuma, P. Salvador, J. J. Dannenberg, D. K. Malick, A. D. Rabuck, K. Raghavachari, J. B. Foresman, J. Cioslowski, J. V. Ortiz, A. G. Baboul, B. B. Stefanov, G. Liu, A. Liashenko, P. Piskorz, I. Komaromi, R. Gomperts, R. L. Martin, D. J. Fox, T. Keith, M. A. Al-Laham, C. Y. Peng, A. Nanayakkara, M. Challacombe, P. M. W. Gill, B. G. Johnson, W. Chen, M. W. Wong, J. L. Andres, C. Gonzalez, M. Head-Gordon, E. S. Replogle and J. A. Pople, *GAUSSIAN 98 (Revision A.11)*, Gaussian, Inc., Pittsburgh, PA, 2001.

39 A. D. Becke, *J. Chem. Phys.*, 1993, **98**, 5648.

40 J. P. Perdew and Y. Wang, *Phys. Rev. B*, 1992, **45**, 13244.

41 D. Andrae, U. Häussermann, M. Dolg, H. Stoll and H. Preuß, *Theor. Chim. Acta*, 1990, **77**, 123.

42 A. W. Ehlers, M. Böhme, S. Dapprich, A. Gobbi, A. Höllwarth, V. Jonas, K. F. Köhler, R. Stegmann, A. Veldkamp and G. Frenking, *Chem. Phys. Lett.*, 1993, **208**, 111.

43 A. Bergner, M. Dolg, W. Küchle, H. Stoll and H. Preuß, *Mol. Phys.*, 1993, **30**, 1431.

44 A. Höllwarth, H. Böhme, S. Dapprich, A. W. Ehlers, A. Gobbi, V. Jonas, K. F. Köhler, R. Stagmann, A. Veldkamp and G. Frenking, *Chem. Phys. Lett.*, 1993, **203**, 237.

45 P. C. Hariharan and J. A. Pople, *Theor. Chim. Acta*, 1973, **28**, 213.